Soleus muscle contains a higher concentration of lipid metabolites than extensor digitorum longus in rats with lipopolysaccharide-induced acute muscle atrophy

Miyoshi, Makoto ; Usami, Makoto ; Nishiyama, Yuya ; Kai, Motoki ; Suzuki, Ayumi ; Maeshige, Noriaki ; Yamaguchi, Atomu ; Ma, Xiaoqi ;…

(Citation)
Clinical Nutrition ESPEN,57:48-57

(Issue Date)
2023-10

(Resource Type)
journal article

(Version)
Accepted Manuscript

Soleus muscle contains a higher concentration of lipid metabolites than extensor digitorum longus in rats with lipopolysaccharide-induced acute muscle atrophy

Makoto Miyoshi,[a] Makoto Usami,[a,b] Yuya Nishiyama,[a] Motoki Kai,[a] Ayumi Suzuki,[a] Noriaki Maeshige,[a] Atomu Yamaguchi,[a] Xiaoqi Ma,[a] Masakazu Shinohara[c,d]

[a] Division of Nutrition and Metabolism, Kobe University Graduate School of Health Sciences, Kobe, Japan

[b] Faculty of Clinical Nutrition and Dietetics, Konan Women's University, Kobe, Japan

[c] The Integrated Center for Mass Spectrometry, Kobe University Graduate School of Medicine, Kobe, Japan

[d] Division of Epidemiology, Kobe University Graduate School of Medicine, Kobe, Japan

Corresponding author:

Makoto Miyoshi, Department of Biophysics, Kobe University Graduate School of Health Sciences, 7-10-2 Tomogaoka, Suma-ku, Kobe 654-0142, Japan

Tel: +81-78-796-4615; Fax: +81-78-796-4509; E-mail: miyoshi@harbor.kobe-u.ac.jp

Abstract

Background & Aims: Muscle atrophy is one of the most important and frequent problems for critically ill patients. The purpose of this study was to evaluate the effect of lipid mediators on acute muscle atrophy. Skeletal muscle fiber-specific analysis of lipid mediators in endotoxemic rats was therefore performed.

Methods: Male Wistar rats were intraperitoneally injected with lipopolysaccharide (LPS). Slow-twitch soleus muscle and fast-twitch extensor digitorum longus (EDL) muscle were harvested 0, 6, and 24 h after LPS injection. Lipid mediators were profiled using liquid chromatography–tandem mass spectrometry, and free fatty acid (FFA) concentrations were measured using gas chromatography–mass spectrometry. Muscles were weighed and their cross-sectional areas were evaluated. Expression levels of mRNAs encoding inflammatory cytokines, autophagy-related transcription factors, and members of the ubiquitin–proteasome system were measured using real-time PCR.

Results: Before LPS injection, the concentrations of all FFAs, including arachidonic acid, eicosapentaenoic acid, and docosahexaenoic acid, and all measured lipid mediators were higher in soleus muscle than in EDL muscle, especially those of pro-inflammatory prostaglandin E_2 (PGE_2) and leukotriene B_4. LPS injection, increased PGE_2 and D_2 and decreased FFAs in soleus muscle but did not change in EDL muscle. The concentrations

of specialized pro-resolving mediators E-series hydroxy-eicosapentaenoic acid and D-series hydroxy-docosahexaenoic acid were higher in soleus muscle. Muscle cross-sectional area decreased and the expression level of atrogin-1 was upregulated in EDL muscle, but both were unchanged in soleus muscle. After LPS injection, a discrepancy involving an increased PGE_2 concentration and decreased muscle atrophy was identified in this acute muscle atrophy model of critical illness.

Conclusion: Concentrations of FFAs and lipid mediators were higher in soleus muscle than in EDL muscle, and LPS injection rapidly increased concentrations of pro-inflammatory lipid mediators. However, muscle atrophy with upregulation of autophagy-related transcription factors was observed in EDL muscle but not in soleus muscle.

Keywords; lipid mediator, skeletal muscle, free fatty acid, lipopolysaccharide, muscle atrophy, muscle fiber type

Introduction

Polyunsaturated fatty acid (PUFA)-derived lipid mediators such as prostaglandins, leukotrienes, lipoxins, resolvins, and protectins play diverse roles in initiation, self-limitation, and active resolution of inflammation [1, 2]. These locally produced chemical signals orchestrate the host response of immune, circulatory, respiratory, gastrointestinal, reproductive, and skeletal muscle systems. Comprehensive analysis of lipid mediators using liquid chromatography–tandem mass spectrometry (LC-MS/MS)-based lipidomics enables simultaneous and quantitative measurements of many lipid mediators [1]. As a source of these mediators, membrane phospholipid PUFAs including arachidonic acid (AA, 20:4 n-6), eicosapentaenoic acid (EPA, 20:5 n-3), and docosahexaenoic acid (DHA, 22:6 n-3) are metabolized by PUFA-oxidizing enzymes such as cyclooxygenase (COX), lipoxygenase (LOX), and cytochrome P450.

Locally produced lipid mediators modulate skeletal muscle inflammation resulting from physical exercise, denervation, various muscular diseases, and critical illness [2, 3]. The roles of AA metabolites including prostaglandins D_2 (PGD_2), E_2, $F_{2\alpha}$, and I_2 and thromboxane B_2 in exercise-induced skeletal muscle injury, together with details of receptors and mechanisms, have been reviewed in detail [4]. A decrease in the concentration of pro-resolving mediators resolvin D1 (RvD1), resolvin E3 (RvE3), and

maresin 1 during maladaptive tissue remodeling in aged mouse muscle was reported, and intraperitoneal injection of RvD1 was shown to control them [5].

Skeletal muscle atrophy occurs in two thirds of patients with sepsis or systemic inflammatory response syndrome [6]. Acquired weakness is a serious complication that significantly worsens the prognosis for patients in intensive care [7]. A rapid loss of muscle mass and strength primarily results from excessive protein breakdown and is accompanied by reduced protein synthesis as a catabolic effect of critical illness [7]. Transcription of genes encoding ubiquitin ligases, such as muscle atrophy F-box (also known as atrogin-1) and muscle RING finger-1 (MuRF1), or encoding autophagy-related transcription factors, such as those in the forkhead box O (FoxO) family and BCL2 interacting protein 3 (Bnip3), account for protein breakdown mediated by ubiquitin proteasomal and autophagic/lysosomal pathways, respectively [8]. A recent in vivo study suggested that lipid mediator control, notably a reduction in prostaglandin E_2 (PGE_2) signaling, plays a significant role in muscle atrophy in sarcopenia with muscle atrophy F-box/atrogin-1 overexpression [9].

Based upon their contractile function, skeletal muscle fibers are often classified as type I, slow oxidative (SO) or type II, fast oxidative glycolytic (FOG) and fast glycolytic (FG) fibers [10, 11]. The degree of muscle wasting can vary among skeletal

muscle subtypes [12], with FG fibers being more vulnerable than SO fibers. Although the differences among phospholipid fatty acids in muscle fiber types could affect their physiological functions and metabolic properties, including contractile function and oxygen efficiency, with varying contributions of subcellular lipid membranes, sarcoplasmic reticulum content, and mitochondrial content [13], no comprehensive within-species study has been reported to determine the fatty acid composition of different lipid mediator-producing skeletal muscle types in a critical illness animal model.

Acute muscle atrophy has been reported in critically ill endotoxemic rats [14-16], the model indicates high responsibility and accumulated knowledge in detailed that pathophysiology [14-18]. The model we used is characterized by a very high concentration of tumor necrosis factor-α (TNF-α) in plasma (24094 pg/mL) 1.5 h after intraperitoneal injection of 10 mg/kg lipopolysaccharide (LPS), with an 87.5% survival rate 24 h post injection [17, 18].

We hypothesized that LPS alters the concentrations of lipid mediators and free fatty acids (FFA) in skeletal muscle. In this study, changes in lipid mediator concentrations in LPS-induced muscle injury were therefore analyzed using LC-MS/MS. Two functionally dissimilar muscles, rat soleus slow muscle, being mainly SO, and extensor digitorum longus (EDL) fast muscle, being mainly FG and FOG, were analyzed

to compare the production of lipid mediators in different skeletal muscle types. Rats are an ideal model because the skeletal muscle profiles of soleus and EDL fibers are surrogates for type I and type II fibers, respectively [10, 11, 19].

Materials and Methods

Animals

Male Wister rats (CLEA Japan, Tokyo, Japan) aged eight weeks and weighing 140–160 g were kept at 22°C under a 12 h light/dark cycle and provided with food and water ad libitum. The day before the experiment, animals (n = 3-5) were provided only with water until they were sacrificed. They were injected intraperitoneally with 10 mg/kg body weight of *Escherichia coli* O111:B4 LPS (Sigma-Aldrich, St. Louis, MO, USA) or saline. Soleus and EDL muscle tissues were collected 0, 6, and 24 h after LPS injection. Although sampling at 24 h has typically been used as to characterize acute inflammation [17, 18], we hypothesized that the earliest changes can be detected 6 h after LPS challenge because MuRF-1 and atrogin-1 are unchanged after 4 h but higher after 8 h [15] and markers of acute inflammation are also changed after 6 h [17, 18]. All procedures for LPS injection, sampling, and sacrifice were performed under anesthesia induced by 1 mg/mL medetomidine (Domitor; Nippon Zenyaku Kogyo, Fukushima, Japan), 5 mg/mL midazolam (Dormicum; Astellas Pharma, Tokyo, Japan), and 5 mg/mL butorphanol (Vetorphale; Meiji Seika Pharma, Tokyo, Japan). This study was approved by the Institutional Animal Care and Use Committee of Kobe University and performed according to the Kobe University Animal Experimentation Regulations (P101208).

Lipid mediator lipidomics

Lipid mediator lipidomics analysis was performed as described previously [20]. Deuterium (d)-labeled internal standards, d_8-5S-hydroxy-eicosatetraenoic acid (5-HETE), d_4-LTB_4, d_5-lipoxin A_4, d_4-PGE_2, and d_5-RvD2 in ice-cold methanol were added to facilitate the quantification of sample recovery. All samples for lipid mediator lipidomics were extracted using C18 solid-phase extraction columns and subjected to LC-MS/MS. The LC-MS/MS system QTrap 6500 (AB Sciex, Tokyo, Japan) was equipped with a Nexera X2 HPLC system (Shimadzu Corporation, Kyoto, Japan). An Agilent Eclipse Plus C18 column (100 mm × 4.6 mm × 1.8 μm) was used with a gradient of methanol:water:acetic acid from 55:45:0.01 (v:v:v) to 98:2:0.01 at a 0.4 mL/min flow rate. To monitor and quantify the levels of targeted lipid mediator, a multiple-reaction monitoring (MRM) method was devised with signature ion fragments for each molecule. Identification was conducted using published criteria using LC retention times, specific fragmentation patterns, and at least six diagnostic fragmentation ions. Quantification was performed based on the peak area of the MRM transition, and linear calibration curves were obtained using an authentic standard for each compound.

Free fatty acid analysis

FFA composition was analyzed using gas chromatography–mass spectrometry (GC-MS). Briefly, total lipids were extracted using the Bligh and Dyer method and FFAs were selectively derivatized to methyl-FAs using trimethylsilyldiazomethane (Tokyo Chemical Industry Co., Tokyo, Japan). Noadecanoic acid (C19:0) was used as an internal standard. Fatty acid methyl esters were analyzed using a GC-MS system (QP2010; Shimadzu, Kyoto, Japan). The capillary column used for fatty acid separation was SP-2650 (100 m×an inner diameter of 0.25 mm×membrane thickness of 0.20 μm; Sigma-Aldrich). The column temperature was maintained at 140°C for 5 min and then increased gradually by 4°C/min to 240°C and held there for 20 min. The sample was injected in split mode with split ratio of 1:5. Each fatty acid methyl ester was detected in selected ion monitoring mode. All results were normalized to the peak height of the C19:0 internal standard.

Total RNA extraction and real-time PCR

Muscle tissues were harvested 0, 6, and 24 h after LPS injection and stored at −80°C until use. Total RNA was extracted from the tissues using TRIzol reagent (Invitrogen, Carlsbad, CA, USA), and 1 mg of extracted total RNA was reverse-

transcribed to yield single-stranded cDNA using an iScript cDNA synthesis kit (Bio-Rad, Hercules, CA, USA). Real-time quantitative PCR analysis (SYBR Green Real time Master Mix; Toyobo, Osaka, Japan) was carried out using a MyiQ detection system (Bio-Rad). The expression levels of mRNAs encoding members of the ubiquitin–proteasome system (atrogin-1 and MuRF1), autophagy-related transcription factors (FoxO1, FoxO3, and Bnip3), and inflammatory cytokines (TNF-α and inducible nitric oxide synthase [iNOS]) were measured. The primer sequences used were: atrogin-1 forward primer 5′-GAACATCATGCAGAGGCTGA-3′ and reverse primer 5′-GTAGCCGGTCTTCACTGAGC-3′; MuRF1 forward primer 5′-ACATCTTCCAGGCTGCCAAT-3′ and reverse primer 5′-GTTCTCCACCAGCAGGTTCC-3′; FoxO1 forward primer 5′-CACACAGCTGGGTGTCAGGCTA-3′ and reverse primer 5′-GGGGTGAAGGGCATCTTT-3′; FoxO3 forward primer 5′-CGGCTCACTTTGTCCCAGAT-3′ and reverse primer 5′-TCTTGCCAGTCCCTTCGTTC-3′; Bnip3 forward primer 5′-CAGAGCGGGGAGGAGAAC-3′ and reverse primer 5′-GAAGCTGGAACGCTGCTC-3′; TNF-α forward primer 5′-CATCTTCTCAAAACTCGAGTGACAA-3′ and reverse primer 5′-

TGGGAGTAGATAAGGTACAGCCC-3′; iNOS forward primer 5′-AACCCAAGGTCTACGTTCAAG-3′ and reverse primer 5′-AAAGTGGTAGCCACATCCCG-3′; glyceraldehyde-3-phosphate dehydrogenase forward primer 5′-GGCACAGTCAAGGCTGAGAATG-3′ and reverse primer 5′-ATGGTGGTGAAGACGCCAGTA-3′.

Relative expression levels of genes were calculated using the ΔΔCt method after normalization to the expression level glyceraldehyde-3-phosphate dehydrogenase and quoted as a fraction of the level immediately prior to LPS injection.

Fiber cross-sectional area (CSA)

Frozen soleus and EDL muscles were cut into 10 μm cross-sections using a cryostat at −20°C. Sections were subjected to myosin ATPase staining at pH 10.4. In this staining (pH 10.4), type I fibers are stained light and type II fibers are dark [21]. The cross-sectional areas of 350 fibers were measured at ×200 magnification using Image J [22].

Statistical analysis

Statistical analysis was performed using Statcel2 software (OMS Publishing Inc., Saitama, Japan). Two-way ANOVA was performed, followed by Tukey–Kramer post hoc analysis. For volcano plots, the fold change of each lipid mediator (soleus/EDL) was calculated and Student's *t*-test was used to evaluate the difference between the abundance of each lipid mediator in soleus and EDL muscles. All parameters are expressed as mean ± standard error of the mean (SEM), and a p value < 0.05 was considered statistically significant.

Results

Lipid mediators and pathway markers

Analyses included a range of n-6 and n-3 PUFA metabolites derived from COX and LOX enzymes (Figure 1). Concentrations of AA metabolites were in the 10–60 pg/mg range, and metabolites of EPA and DHA were detected at relatively lower concentrations.

Before and after LPS injection, concentrations of all measured lipid mediators were higher in soleus muscle than in EDL muscle. The concentrations of pro-inflammatory PGE_2, an AA metabolite, were 9.52 pg/mg in soleus muscle and 2.58 pg/mg in EDL muscle and increased 4.4-fold to 42.28 pg/mg in soleus muscle 6 h after LPS injection and 5.2-fold to 13.54 pg/mg in EDL muscle 24 h post injection ($p < 0.01$, Figure 1).The concentrations of leukotriene B_4, a LOX-derived metabolite of AA, were 0.38 pg/mg in soleus muscle and 0.02 pg/mg in EDL muscle ($p < 0.05$) and decreased after LPS injection in soleus muscle (NS, Figure 1). There were no notable changes in thromboxane B_2 concentration. AA-derived pathway markers lipoxin B_4 and 5-, 12-, and 15-HETEs in soleus muscle were higher than their respective values in EDL muscle before and after LPS injection ($p < 0.05$, Figure 1). Concentrations of anti-inflammatory RvE3, an EPA metabolite, were 0.04 pg/mg in soleus muscle and 0.00 pg/mg in EDL muscle (NS, Figure 2). Concentrations of EPA-derived pathway markers 5-, 12-, 15-, and

18-hydroxy-eicosapentaenoic acids (HEPEs) were also higher in soleus muscle than in EDL muscle ($p < 0.01–0.05$, Figure 2). DHA-derived anti-inflammatory lipid mediators resolvin D5 (RvD5) (0.18 pg/mg) and protectin D1 (0.04 pg/mg) were detected in soleus muscle but below the detection limit in EDL muscle (Figure 3). The concentrations of DHA-derived pathway markers 7-, 14-, and 17 hydroxy-docosahexaenoic acids (HDHAs) were higher in soleus muscle before and after LPS injection ($p < 0.05$, Figure 3).

Volcano plots were used to analyze lipid mediator concentrations and showed that they were higher in soleus muscle than in EDL muscle at 0, 6, and 24 h after LPS injection, the largest difference being measured 6 h post injection (Figure 4).

Free fatty acids

Before LPS injection, almost all FFA concentrations were higher in soleus muscle than in EDL muscle (Figure 5, Table 1), especially those of total fatty acids (2.9-fold, $p < 0.01$), PUFAs (3.6-fold, $p < 0.01$), AA (5.5-fold, $p < 0.01$), EPA (4.8-fold, $p < 0.01$), DHA (3.1-fold, $p < 0.05$), saturated fatty acids (SFAs; 2.0-fold, $p < 0.01$) and monounsaturated fatty acids (2.7-fold, $p < 0.01$). After LPS injection, the concentrations of the above FFAs decreased, with those of AA, EPA, and DHA decreasing more in soleus muscle than in EDL muscle ($p < 0.01–0.05$, Figure 5, Table 1).

Skeletal muscle mass, CSA, TNF-α, ubiquitin–proteasome proteins, and autophagy-related transcription factors

EDL muscle mass decreased from 0.43 ± 0.01 mg/g body weight to 0.38 ± 0.00 mg/g 24 h after LPS injection ($p < 0.05$, Figure 6A). However, soleus muscle mass (0.40 ± 0.01 mg/g) was not significantly decreased 24 h post injection compared with that before LPS treatment (0.43 ± 0.02 mg/g). The mean CSA of EDL muscle (type II fibers) decreased from 2436.9 ± 16.3 μm^2 to 1468.6 ± 221.2 μm^2 24 h after LPS injection ($p < 0.01$, Figure 6B, C). In contrast, the CSA of soleus muscle fibers was the same before (type I, 1949.8 ± 70.4 μm^2; type II, 1332.4 ± 135.2 μm^2) and 24 h after (type I, 1866.3 ± 119.5 μm^2; type II 1332.0 ± 81.6 μm^2) LPS injection. The CSA of EDL (type II) muscle fibers was larger than that of soleus (type I and II) muscle fibers before LPS injection ($p < 0.01$, Figure 6B).

Higher expression of TNF-α mRNA was measured in soleus muscle and EDL muscle 6 h and 24 h, respectively, after LPS treatment (NS, Figure 7). Atrogin-1 and MuRF1 mRNAs in the ubiquitin–proteasome system were upregulated in EDL muscle 6 h and 24 h after LPS injection, whereas their respective expression levels in soleus muscle were unchanged and significantly lower than those in EDL muscle ($p < 0.05$, Figure 8).

Expression levels of mRNAs encoding autophagy-related transcription factors FoxO1, FoxO3, and Bnip3 were upregulated in soleus muscle 6 h post LPS injection (NS, Figure 8) and returned to their pre-treatment levels after 24 h. Upregulation of Bnip3 mRNA in soleus muscle was higher than that in EDL muscle 6 h post LPS injection, but the difference was not significant.

Discussion

To our knowledge, this is the first study to comprehensively investigate changes in concentrations of lipid mediators and FFAs in two functionally dissimilar skeletal muscle fibers, soleus (slow-twitch, type I oxidative) and EDL (fast-twitch, type II glycolytic) muscle fibers, before and after LPS injection. FFA concentrations were higher in soleus muscle than in EDL muscle, consistent with higher concentrations of lipid mediators, especially pro-inflammatory PGD_2, PGE_2 and the specialized pro-resolving mediators (SPMs) E-series HEPE and D-series HDHA, a key finding in this study. Concentrations of AA, EPA, and DHA, a precursor pool for lipid mediators, decreased in soleus muscle after LPS injection in accordance with increased lipid mediator concentrations. After LPS injection, muscle CSA decreased and expression of mRNA encoding ubiquitin ligase atrogin-1 was upregulated in EDL muscle but not in soleus muscle.

Our finding that the constitutive PGE_2 concentration in soleus muscle is higher than that in EDL muscle is in agreement with some reports. Only one human study found that concentrations of PGE_2 and PGE_2/COX pathway enzymes and receptors are higher in soleus muscle than in vastus lateralis (type II) fast muscle fibers [23]. Regarding the effect of FFA on lipid mediators, SFAs upregulate skeletal muscle COX activity in C2C12

cell culture [24] and thus the 2-fold higher SFA in soleus muscle might likewise upregulate COX activity and PGE_2 concentration in this muscle. FFAs are the energy source in oxidative soleus muscle because of metabolic requirements in type I muscle [13]. Soleus muscle has a higher capillary volume and capillary-to-fiber ratio than in EDL muscle [25]. Capillary endothelium synthesizes lipoprotein-lipase, and a larger capillary volume results in a larger contribution of lipoprotein-lipase activity to the supply of fatty acids and their oxidation in response to energy demand in soleus muscle [26]. Thus, sufficient FFA is essential to form fatty acid-derived bioactive lipid mediators [27], which is in accordance with our finding that concentrations of source PUFAs consisting of AA, EPA, and DHA decreased commensurately with an increase in lipid mediator concentrations in soleus muscle after LPS injection.

As for LPS-induced changes in pro-resolving mediators, the concentration of RvE3, an omega-3 PUFA-derived SPM, was significantly higher than that in EDL muscle at 24 h, while those of RvD5 and PD1, omega-6 PUFA-derived SPMs, were suspected to be higher in soleus muscle. The concentration of 18-HEPE, a pathway marker for the formation of anti-inflammatory E-resolvins [28], was significantly higher in soleus muscle. The concentration of DHA-derived D-series resolvin pathway marker 17-HDHA and maresin precursor 14-HDHA [29] were also significantly higher in soleus muscle

compared with EDL muscle. Some concentrations were constitutively higher, whereas some were higher after LPS injection. As far as we know, the in vivo changes of SPMs in skeletal muscle have not previously been reported, but their anti-inflammatory, pro-resolving, microbial clearing, anti-thrombotic, and organ-protective actions in soleus muscle could be useful and contribute to muscle damage prevention. The above measured changes in lipid mediators and FFAs provide support for their role in skeletal muscle pathophysiology during critical illness.

Our results of muscle atrophy agrees with many reports on critical illness induced by LPS or TNF-α injection in rats [14-16]. Protein synthesis is not changed in the early phase after LPS challenge, and no change after 24 h in the anabolic molecule mTOR in gastrocnemius type II fibers was reported [30]. At first, we hypothesized that a higher pro-inflammatory lipid mediator concentration would evoke acute muscle atrophy [2], but we obtained the opposite result, with less muscle atrophy being measured in soleus muscle than in EDL muscle 24 h after LPS injection. Our finding that greater upregulation of atrogin-1 occurs in EDL muscle than in soleus muscle is in accordance with the assertion that type II fibers atrophy more than type I fibers with sepsis [12]. In addition, PGE_2, a typical pro-inflammatory lipid mediator, is involved in muscle regeneration but not atrophy signaling [5, 31]. Also, the characteristics of soleus muscle

as a slow or antigravity muscle [32] may affect its tolerance to pro-inflammatory factors, including lipid mediators. A study of fiber type-specific atrophy indicated that oxidative soleus muscle has higher iNOS and antioxidant enzyme activities and greater protection against muscle atrophy than white vastus lateralis, a type II glycolytic muscle similar to EDL muscle [33]. Furthermore, increased PGE_2 might contribute to muscle regeneration longer time after LPS injection. Further research is required to understand lipid mediator control of acute muscle atrophy induced by sepsis or systemic inflammatory response syndrome.

Regarding lipid mediators in other pathophysiologic conditions, muscle atrophy due to cachectic stimulation [33], a reduction in PGE_2 signaling was found to be a major contributor to chronic muscle atrophy in aged mice during a one-month period of skeletal muscle repair and regeneration [10]. Lipid signaling mediators contribute to skeletal muscle myogenesis, repair, and regeneration [34]. Changes in the concentration of receptors and parent enzymes of dynamic lipid mediators occur during skeletal muscle regeneration after cardiotoxin injury, and RvD2 increases the number of immune cells in skeletal muscle [35]. An acute bout of resistance exercise in human vastus lateralis leads to a transient increase in many lipid mediators [36]. However, the magnitude of the increase (2.8 pg/mg of PGE_2 during exercise) is much lower than that measured in this

study (40 pg/mg). Moreover, the increase in PGE_2 concentration peaked 2 h after exercise and then returned to the resting value after 4 h, but it peaked 6 h after LPS injection and remained high after 24 h. A persistently high PGE_2 concentration in skeletal muscle during the latter septic condition would lead to prominent and characteristic effects.

A limitation of this study is that we did not elucidate a detailed mechanism underpinning the changes in lipid mediator concentrations during acute illness. Lipid mediators come from LPS-stimulated resident immune cells, including monocyte-macrophages, and neutrophils in this acute illness model then affect muscle cells [37]. Detailed and specific analysis in those cross-talk will be required for future research including newly discovered SPMs to understand skeletal muscle pathophysiology [27]. Long-term follow-up after acute muscle atrophy with muscle regeneration, resolution phase in lipid mediator production, has not been evaluated in this experimental model [27]. Identification of changes in lipid mediator concentrations in skeletal muscle is expected to lead to the elucidation of the pathogenesis of secondary muscle atrophy and development of new prevention and treatment strategies. These strategies may include: 1) control of lipid mediators by exogenous SPM administration [5] or inhibition of specific enzymes [10]; 2) nutritional interventions using omega-3 PUFA, EPA, and/or DHA, which can change skeletal muscle phospholipid fatty acids and their functional

response [38-40]; 3) introduction of fiber type-specific COX-inhibiting drugs that exploit the fundamentally different contractile and metabolic characteristics of each fiber type [41].

Conclusion

Constitutively higher FFAs concentrations in soleus type I oxidative muscle fiber than in EDL type II glycolytic muscle fiber were revealed, suggesting a metabolic requirement in slow muscle for an energy source. Sufficient FFA is essential to form fatty acid derived bioactive lipid mediators and source PUFAs were decreased with increase of lipid mediators after LPS injection in soleus muscle. LPS injection rapidly increased concentrations of pro-inflammatory mediators and SPMs in soleus muscle but not in EDL muscle. However, muscle atrophy, with upregulation of autophagy-related transcription factors, was observed in EDL but not soleus muscle, suggesting lipid mediators did not induce muscle regeneration in this very early phase of acute illness. Future lipid metabolite research is required in pathophysiology of skeletal muscle fibers.

Funding statement

This work was partially supported by JSPS KAKENHI (Grant-in-Aid for Scientific

Research), Grant Number 25450450.

Conflict of Interest Statement

We have no conflicts of interest with respect to any financial matters or personal relationships.

Author Contributions

MM: Conceptualization, Methodology, Data curation, Visualization, Writing-Original draft preparation, Reviewing and Editing. MU: Conceptualization, Methodology, Writing-Original draft preparation, Reviewing and Editing. YN, MK, AS, NM, and MS: Investigation. AY and XM: Data curation.

References

[1] Arita M. Mediator lipidomics in acute inflammation and resolution. J Biochem 2012; 152: 313-9.

[2] Korotkova M, Lundberg IE. The skeletal muscle arachidonic acid cascade in health and inflammatory disease. Nat Rev Rheumatol 2014; 10: 295-303.

[3] Cheng H, Huang H, Guo Z, Chang Y, Li Z. Role of prostaglandin E2 in tissue repair and regeneration. Theranostics 2021; 11: 8836-54.

[4] Markworth JF, Maddipati KR, Cameron-Smith D. Emerging roles of pro-resolving lipid mediators in immunological and adaptive responses to exercise-induced muscle injury. Exerc Immunol Rev 2016; 22: 110-34.

[5] Markworth JF, Brown LA, Lim E, Castor-Macias JA, Larouche J, Macpherson PCD, et al. Metabolipidomic profiling reveals an age-related deficiency of skeletal muscle pro-resolving mediators that contributes to maladaptive tissue remodeling. Aging Cell 2021; 20: e13393.

[6] Koukourikos K, Tsaloglidou A, Kourkouta L. Muscle atrophy in intensive care unit patients. Acta Inform Med 2014; 22: 406-10.

[7] Maestraggi Q, Lebas B, Clere-Jehl R, Ludes PO, Chamaraux-Tran TN, Schneider F, et al. Skeletal muscle and lymphocyte mitochondrial dysfunctions in septic shock trigger

ICU-acquired weakness and sepsis-induced immunoparalysis. Biomed Res Int 2017; 2017: 7897325.

[8] Fanzani A, Conraads VM, Penna F, Martinet W. Molecular and cellular mechanisms of skeletal muscle atrophy: an update. J Cachexia Sarcopenia Muscle 2012; 3: 163-79.

[9] Palla AR, Ravichandran M, Wang YX, Alexandrova L, Yang AV, Kraft P, et al. Inhibition of prostaglandin-degrading enzyme 15-PGDH rejuvenates aged muscle mass and strength. Science 2021; 371: eabc8059.

[10] Westerblad H, Bruton JD, Katz A. Skeletal muscle: energy metabolism, fiber types, fatigue and adaptability. Exp Cell Res 2010; 316:3093-9.

[11] Armstrong RB, Phelps RO. Muscle fiber type composition of the rat hindlimb. Am J Anat 1984; 171: 259-72.

[12] Wang Y, Pessin JE. Mechanisms for fiber-type specificity of skeletal muscle atrophy. Curr Opin Clin Nutr Metab Care 2013; 16: 243-50.

[13] Abbott SK, Else PL, Atkins TA, Hulbert AJ. Fatty acid composition of membrane bilayers: importance of diet polyunsaturated fat balance. Biochim Biophys Acta 2012; 1818: 1309-17.

[14] Murton AJ, Alamdari N, Gardiner SM, Constantin-Teodosiu D, Layfield R, Bennett T, et al. Effects of endotoxaemia on protein metabolism in rat fast-twitch skeletal muscle and myocardium. PLoS One 2009; 4: e6945.

[15] Frost RA, Nystrom GJ, Jefferson LS, Lang CH. Hormone, cytokine, and nutritional regulation of sepsis-induced increases in atrogin-1 and MuRF1 in skeletal muscle. Am J Physiol Endocrinol Metab 2007; 292: E501-12.

[16] Lang CH, Silvis C, Deshpande N, Nystrom G, Frost RA. Endotoxin stimulates in vivo expression of inflammatory cytokines tumor necrosis factor alpha, interleukin-1beta, -6, and high-mobility-group protein-1 in skeletal muscle. Shock 2003; 19: 538-46.

[17] Miyoshi M, Sakaki H, Usami M. Iizuka N, Shuno K, Aoyama M, et al. Oral administration of tributyrin increases concentration of butyrate in the portal vein and prevents lipopolysaccharide-induced liver injury in rats. Clin Nutr 2011; 30: 252-8.

[18] Miyoshi M, Iizuka N, Sakai S, Fujiwara M, Aoyama-Ishikawa M, Maeshige N, et al. Oral tributyrin prevents endotoxin-induced lipid metabolism disorder. Clin Nutr ESPEN 2015; 10: e83-8.

[19] Ohlendieck K. Proteomics of skeletal muscle glycolysis. Biochim Biophys Acta 2010; 1804: 2089-101.

[20] Colas RA, Shinohara M, Dalli J, Chiang N, Serhan CN. Identification and signature profiles for pro-resolving and inflammatory lipid mediators in human tissue. Am J Physiol Cell Physiol 2014; 307: C39-54.

[21] Nishida H, Ikegami A, Kaneko C, Kakuma H, Nishi H, Tanaka N, et al. Dexamethasone and BCAA failed to modulate muscle mass and mTOR signaling in GH-deficient rats. PLoS One 2015; 10: e0128805.

[22] Schneider CA, Rasband WS, Eliceiri KW. NIH Image to ImageJ: 25 years of image analysis. Nature Methods 2012; 9: 671–5.

[23] Liu SZ, Jemiolo B, Lavin KM, Lester BE, Trappe SW, Trappe TA. Prostaglandin E2/cyclooxygenase pathway in human skeletal muscle: influence of muscle fiber type and age. J Appl Physiol (1985) 2016; 120: 546-51.

[24] Kadotani A, Tsuchiya Y, Hatakeyama H, Katagiri H, Kanzaki M. Different impacts of saturated and unsaturated free fatty acids on COX-2 expression in C(2)C(12) myotubes. Am J Physiol Endocrinol Metab 2009; 297: E1291-303.

[25] Murakami S, Fujino H, Takeda I, Momota R, Kumagishi K, Ohtsuka A. Comparison of capillary architecture between slow and fast muscles in rats using a confocal laser scanning microscope. Acta med Okayama 2010; 64; 11-8.

[26] Hall G. The physiological regulation of skeletal muscle fatty acid supply and oxidation during moderate-intensity exercise. Sports Med 2015; 45: S23-32.

[27] Dyall SC, Balas L, Bazan NG, Brenna JT, Chiang N, Souza FC, et al. Polyunsaturated fatty acids and fatty acid-derived lipid mediators: Recent advances in the understanding of their biosynthesis, structures, and functions. Prog Lipid Res 2022; 86: 101165.

[28] Weylandt KH, Chiu CY, Gomolka B, Waechter SF, Wiedenmann B. Omega-3 fatty acids and their lipid mediators: towards an understanding of resolvin and protectin formation. Prostaglandins Other Lipid Mediat 2012; 97: 73-82.

[29] Mozurkewich EL, Greenwood M, Clinton C, Berman D, Romero V, Djuric Z, et al. Pathway markers for pro-resolving lipid mediators in maternal and umbilical cord blood: a secondary analysis of the mothers, omega-3, and mental health study. Front Pharmacol 2016; 7: 274.

[30] Valentine RJ, Jefferson MA, Kohut ML, Eo H. Imoxin attenuates LPS-induced inflammation and MuRF1 expression in mouse skeletal muscle. Physiol Rep 2018; 6: e13941.

[31] Cheng H, Huang H, Guo Z, Chang Y, Li Z. Role of prostaglandin E2 in tissue repair and regeneration. Theranostics 2021; 11: 8836-54.

[32] Zhang P, Chen X, Fan M. Signaling mechanisms involved in disuse muscle atrophy. Med Hypotheses 2007; 69: 310-21.

[33] Yu Z, Li P, Zhang M, Hannink M, Stamler JS, Yan Z. Fiber type-specific nitric oxide protects oxidative myofibers against cachectic stimuli. PLoS One 2008; 3: e2086.

[34] Mo C, Wang Z, Bonewald L, Brotto M. Multi-staged regulation of lipid signaling mediators during myogenesis by COX-1/2 pathways. Int J Mol Sci 2019; 20: 4326.

[35] Giannakis N, Sansbury BE, Patsalos A, Hays TT, Riley CO, Han X, et al. Dynamic changes to lipid mediators support transitions among macrophage subtypes during muscle regeneration. Nat Immunol 2019; 20: 626-36.

[36] Vella L, Markworth JF, Farnfield MM, Maddipati KR, Russell AP, Cameron-Smith D. Intramuscular inflammatory and resolving lipid profile responses to an acute bout of resistance exercise in men. Physiol Rep 2019; 7: e14108.

[37] Pillon NJ, Bilan PJ, Fink LN, Klip A. Cross-talk between skeletal muscle and immune cells: muscle-derived mediators and metabolic implications. Am J Physiol Endocrinol Metab 2013; 304: E453-65.

[38] Jeromson S, Gallagher IJ, Galloway SD, Hamilton DL. Omega-3 fatty acids and skeletal muscle health. Mar Drugs 2015; 13: 6977-7004.

[39] Macartney MJ, Peoples GE, Treweek TM, McLennan PL. Docosahexaenoic acid varies in rat skeletal muscle membranes according to fibre type and provision of dietary fish oil. Prostaglandins Leukot Essent Fatty Acids 2019; 151: 37-44.

[40] Liu Y, Chen F, Odle J, Lin X, Zhu H, Shi H, et al. Fish oil increases muscle protein mass and modulates Akt/FOXO, TLR4, and NOD signaling in weanling piglets after lipopolysaccharide challenge. J Nutr 2013; 143: 1331-9.

[41] Trappe TA, Liu SZ. Effects of prostaglandins and COX-inhibiting drugs on skeletal muscle adaptations to exercise. J Appl Physiol (1985) 2013; 115: 909-19.

Figure Legends

Figure 1. AA-derived lipid concentrations (pg/mg) in soleus (closed squares, dashed line) and EDL (diamonds, solid line) muscles 0, 6, and 24 h after LPS injection.

Values represent the mean ± SEM of 4 animals per group at each time point. $^{\#}p < 0.05$, $^{\#\#}p < 0.01$ versus soleus muscle at 0 h; $^{*}p < 0.05$, $^{**}p < 0.01$ soleus muscle versus EDL muscle. *P* values indicated the results of two-way ANOVA with time (0, 6, 24 h) and group (soleus versus EDL) as factors. Individual data points are shown (soleus muscle, open circles; EDL muscle, open squares). AA, arachidonic acid; EDL, extensor digitorum longus; LPS, lipopolysaccharide; PGD_2, prostaglandin D_2; PGE_2, prostaglandin E_2; $PGF_{2\alpha}$, prostaglandin $F_{2\alpha}$; PGH_2, prostaglandin H_2; TxB_2, thromboxane B_2; COX-2, cyclooxygenase-2 ; LOX, lipoxygenase; ETE, eicosatetraenoic acid; HETE, hydroxy-eicosatetraenoic acid; HpETE, hydroperoxyeicosatetraenoic acid; LTA_4, leukotriene A_4; LTB_4, leukotriene B_4; LXA_4, lipoxin A_4; LXB_4, lipoxin B_4.

Figure 2. EPA-derived lipid mediator concentrations (pg/mg) in soleus (closed squares, dashed line) and EDL (diamonds, solid line) muscles 0, 6, and 24 h after LPS injection.

Values represent the mean ± SEM of 4 animals per group at each time point. $^{*}p < 0.05$, $^{**}p < 0.01$ soleus muscle versus EDL muscle. *P* values indicated the results of two-way

ANOVA with time (0, 6, 24 h) and group (soleus versus EDL) as factors. Individual data points are shown (soleus muscle, open circles; EDL muscle, open squares). EPA, eicosapentaenoic acid; HEPE, hydroxy-eicosapentaenoic acid; HpEPE, hydroperoxyeicosapentaenoic acid; P450, cytochrome P450; RvE1, resolvin E1; RvE2, resolvin E2; RvE3, resolvin E3.

Figure 3. DHA-derived lipid mediator concentrations (pg/mg) in soleus (closed squares, dashed line) and EDL (diamonds, solid line) muscles 0, 6, and 24 h after LPS injection. Values represent the mean ± SEM of 4 animals per group at each time point. $^{*}p < 0.05$ soleus muscle versus EDL muscle. *P* values indicated the results of two-way ANOVA with time (0, 6, 24 h) and group (soleus versus EDL) as factors. Individual data points are shown (soleus muscle, open circles; EDL muscle, open squares). DHA, docosahexaenoic acid; HDHA, hydroxy-docosahexaenoic acid; HpDHA, hydroperoxydocosahexaenoic acid; RvD1, resolvin D1; RvD2, resolvin D2; RvD3, resolvin D3; RvD5, resolvin D5; PD1, protectin D1; MaR1, maresin 1.

Figure 4. Volcano plots summarizing the magnitude and statistical significance of differences between soleus and EDL muscle concentrations of individual lipid mediators 0, 6, and 24 h after LPS injection.

The horizontal axis shows the $\log_2$-fold difference between soleus and EDL muscle concentrations and the vertical axis shows the value of $-\log_{10}p$. As the threshold, the vertical lines indicate fold change = 2 or 0.5 and the horizontal lines indicate $-\log_{10}$p = 1 ($p = 0.1$). Red dots indicate fold changes > 2 with $p < 0.1$.

Figure 5. Free fatty acid concentrations (pmol/mg) in soleus (closed squares, dashed line) and EDL (diamonds, solid line) muscles 0, 6, and 24 h after LPS injection.

Values represent the mean ± SEM of 4 animals per group at each time point. $^{\#}p < 0.05$, $^{\#\#}p < 0.01$ versus soleus muscle at 0 h; $^{*}p < 0.05$, $^{**}p < 0.01$ soleus muscle versus EDL muscle. *P* values indicated the results of two-way ANOVA with time (0, 6, 24 h) and group (soleus versus EDL) as factors. Individual data points are shown (soleus muscle, open circles; EDL muscle, open squares). AA, arachidonic acid; EPA, eicosapentaenoic acid; DHA, docosahexaenoic acid.

Figure 6. Time-dependent effects of LPS on muscle mass and CSA.

A) Muscle mass. B) CSA. C) Density plot of the CSA. D) ATPase staining (pH 10.4) of soleus and EDL muscle fibers (type I fibers are appear light, and type II fibers appear dark). Scale bar: 100 μm. Values represent the mean ± SEM of 3-4 animals per group at each time point. $^{\$}p < 0.05$ versus EDL muscle at 0 h; $^{**}p < 0.01$ soleus muscle versus EDL muscle. *P* values indicated the results of two-way ANOVA with time (0, 6, 24 h) and group (soleus versus EDL) as factors. Individual data points are shown (soleus muscle, open circles; EDL muscle, open squares). CSA, cross-sectional area; I, type I slow oxidative fibers; II, type II fast oxidative glycolytic and fast glycolytic fibers.

Figure 7. Relative expression of mRNAs encoding TNF-α and iNOS in soleus (closed squares, dashed line) and EDL (diamonds, solid line) muscles 0, 6, and 24 h after LPS injection.

Values represent the mean ± SEM of 3-5 animals per group at each time point. *P* values indicated the results of two-way ANOVA with time (0, 6, 24 h) and group (soleus versus EDL) as factors. Individual data points are shown (soleus muscle, open circles; EDL muscle, open squares). TNF-α, tumor necrosis factor-α; iNOS; inducible nitric oxide synthase.

Figure 8. Relative expression of mRNAs encoding members of the ubiquitin–proteasome system and autophagy transcriptional factors in soleus (closed squares, dashed line) and EDL (diamonds, solid line) muscles 0, 6, and 24 h after LPS injection.

Values represent the mean ± SEM of 3-5 animals per group at each time point. $^{\$}p < 0.05$ versus EDL muscle at 0 h; $^{*}p < 0.05$ soleus muscle versus EDL muscle. *P* values indicated the results of two-way ANOVA with time (0, 6, 24 h) and group (soleus versus EDL) as factors. Individual data points are shown (soleus muscle, open circles; EDL muscle, open squares). FoxO1, forkhead box O1; FoxO3, forkhead box O3; MuRF1, muscle RING finger-1; Bnip3, BCL2 interacting protein 3.

Figure 1

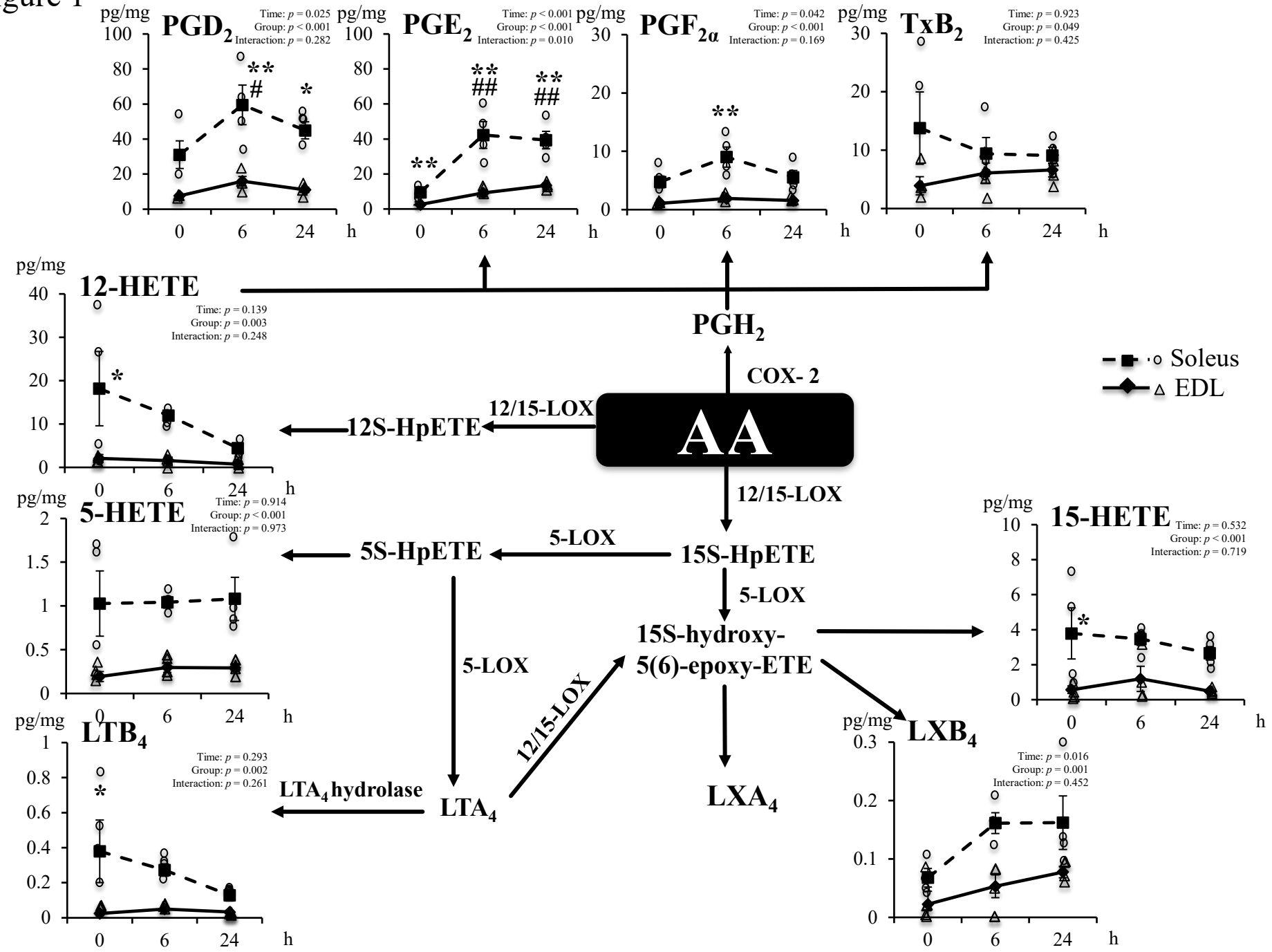
pg/mg
PGD2
Time: p = 0.025
Group: p < 0.001
Interaction: p = 0.282
PGE2
Time: p < 0.001
Group: p < 0.001
Interaction: p = 0.010
PGF2α
Time: p = 0.042
Group: p < 0.001
Interaction: p = 0.169
TxB2
Time: p = 0.923
Group: p = 0.049
Interaction: p = 0.425
12-HETE
Time: p = 0.139
Group: p = 0.003
Interaction: p = 0.248
PGH2
COX- 2
12/15-LOX
12S-HpETE
AA
12/15-LOX
Soleus
EDL
5-HETE
Time: p = 0.914
Group: p < 0.001
Interaction: p = 0.973
5S-HpETE
5-LOX
15S-HpETE
15-HETE
Time: p = 0.532
Group: p < 0.001
Interaction: p = 0.719
5-LOX
15S-hydroxy-
5(6)-epoxy-ETE
5-LOX
12/15-LOX
LTB4
Time: p = 0.293
Group: p = 0.002
Interaction: p = 0.261
LTA4 hydrolase
LTA4
LXA4
LXB4
Time: p = 0.016
Group: p = 0.001
Interaction: p = 0.452
h

Figure 2

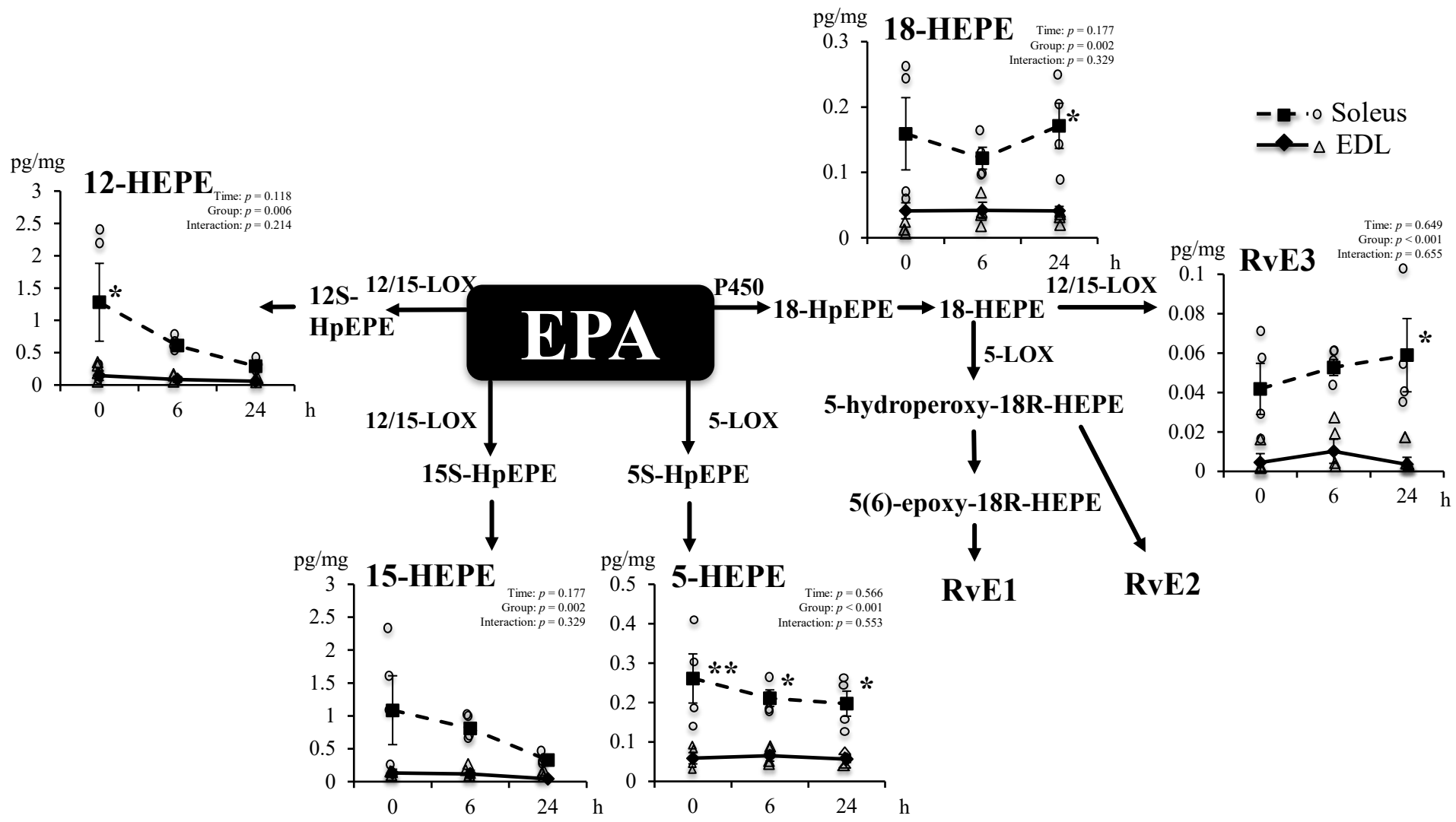
EPA
12/15-LOX
12S-HpEPE
12-HEPE
Time: p = 0.118
Group: p = 0.006
Interaction: p = 0.214
pg/mg
h
P450
18-HpEPE
18-HEPE
Time: p = 0.177
Group: p = 0.002
Interaction: p = 0.329
Soleus
EDL
12/15-LOX
RvE3
Time: p = 0.649
Group: p < 0.001
Interaction: p = 0.655
5-LOX
5-hydroperoxy-18R-HEPE
12/15-LOX
5-LOX
15S-HpEPE
5S-HpEPE
5(6)-epoxy-18R-HEPE
15-HEPE
Time: p = 0.177
Group: p = 0.002
Interaction: p = 0.329
5-HEPE
Time: p = 0.566
Group: p < 0.001
Interaction: p = 0.553
RvE1
RvE2

Figure 3

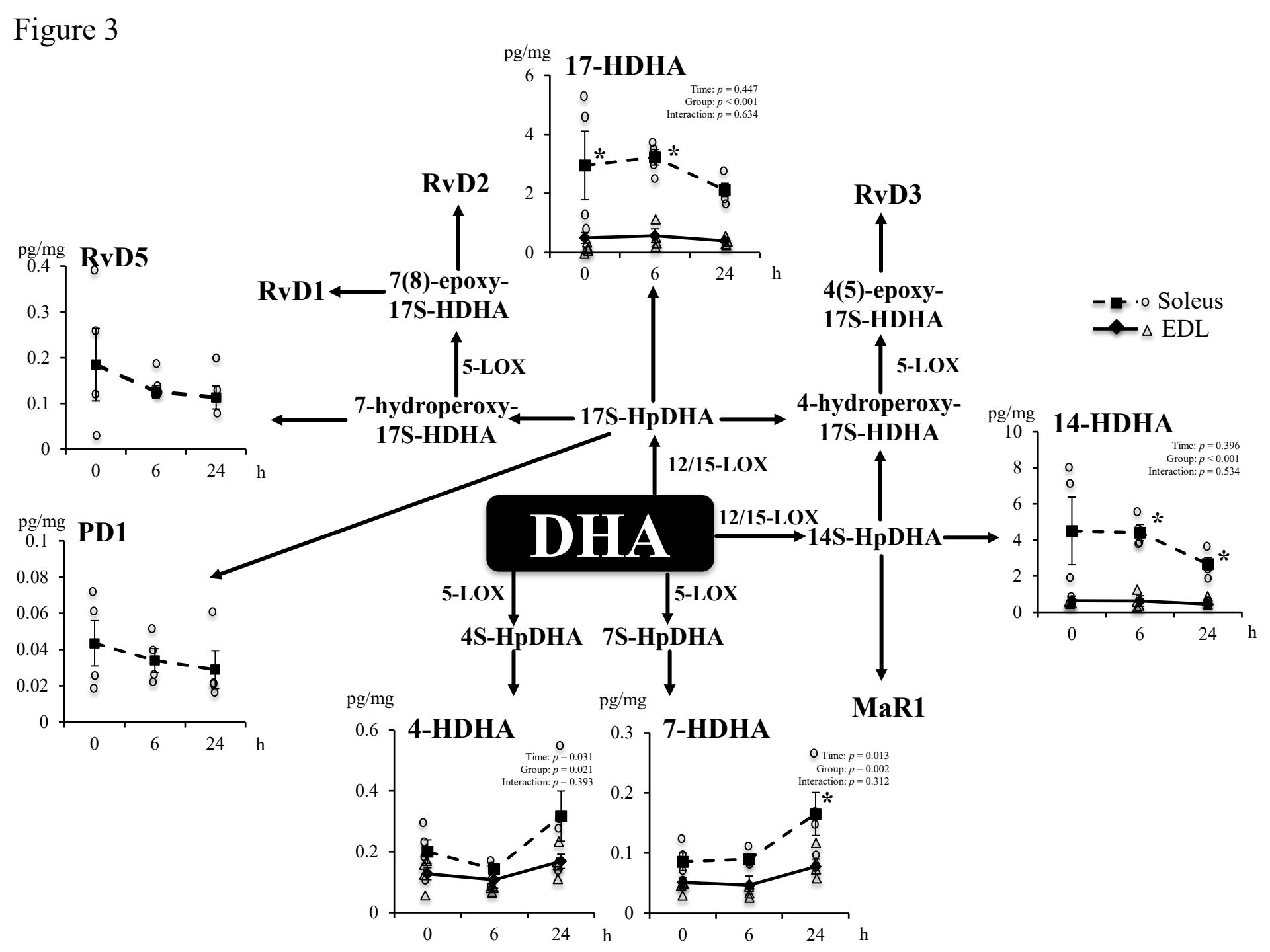
DHA
12/15-LOX
5-LOX
17S-HpDHA
7-hydroperoxy-17S-HDHA
4-hydroperoxy-17S-HDHA
14S-HpDHA
4S-HpDHA
7S-HpDHA
7(8)-epoxy-17S-HDHA
4(5)-epoxy-17S-HDHA
RvD1
RvD2
RvD3
RvD5
PD1
MaR1
17-HDHA
14-HDHA
4-HDHA
7-HDHA
pg/mg
Time: p = 0.447
Group: p < 0.001
Interaction: p = 0.634
Time: p = 0.396
Group: p < 0.001
Interaction: p = 0.534
Time: p = 0.031
Group: p = 0.021
Interaction: p = 0.393
Time: p = 0.013
Group: p = 0.002
Interaction: p = 0.312
Soleus
EDL
h

Figure 4

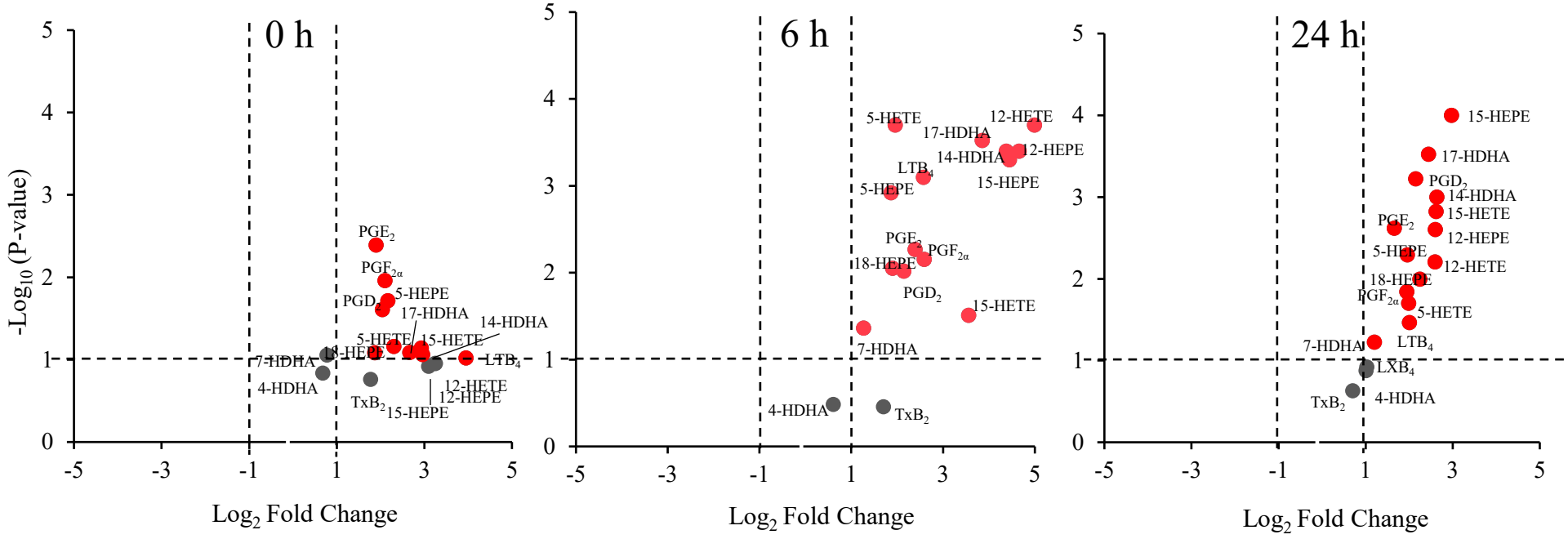
0 h
6 h
24 h
-Log10 (P-value)
Log2 Fold Change
PGE2
PGF2α
PGD2
5-HEPE
17-HDHA
14-HDHA
5-HETE
15-HETE
18-HEPE
7-HDHA
LTB4
4-HDHA
TxB2
12-HETE
12-HEPE
15-HEPE
LXB4

Figure 5

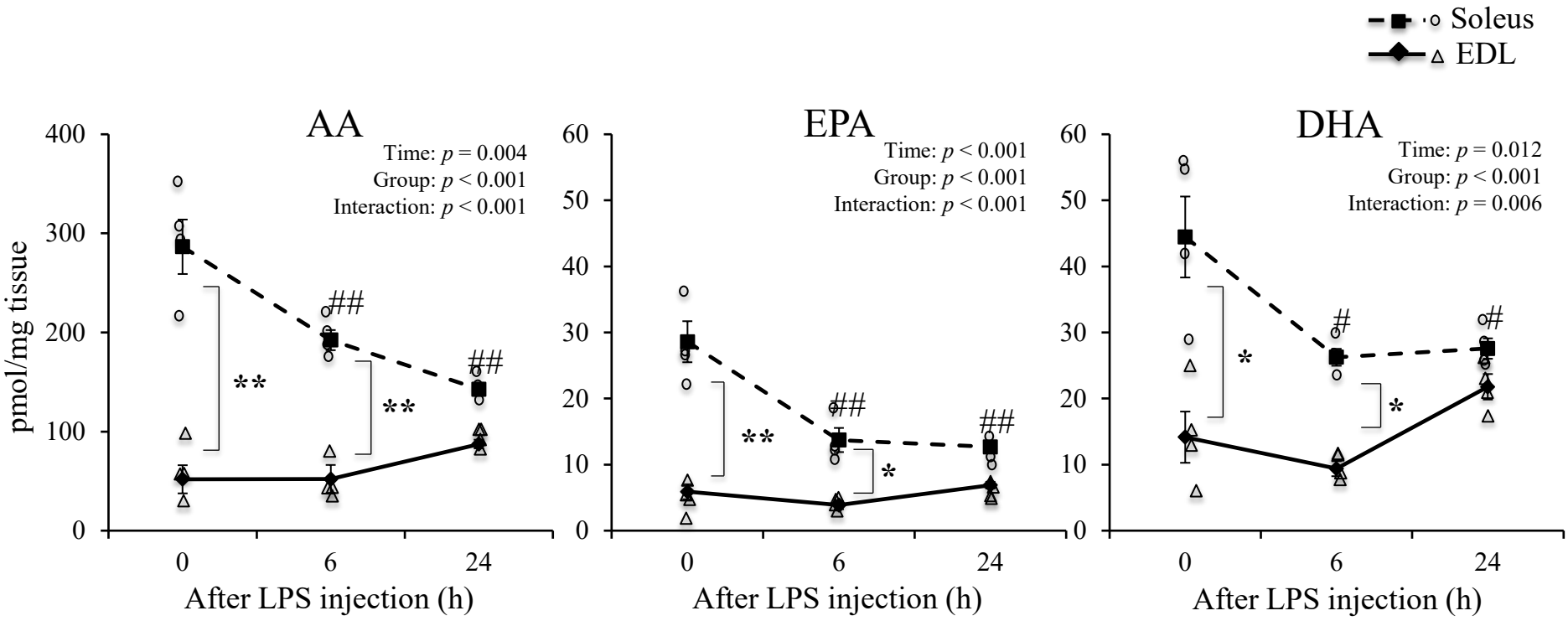
Soleus
EDL
AA
Time: $p = 0.004$
Group: $p < 0.001$
Interaction: $p < 0.001$
EPA
Time: $p < 0.001$
Group: $p < 0.001$
Interaction: $p < 0.001$
DHA
Time: $p = 0.012$
Group: $p < 0.001$
Interaction: $p = 0.006$
pmol/mg tissue
After LPS injection (h)
0
6
24
##
#
**
*

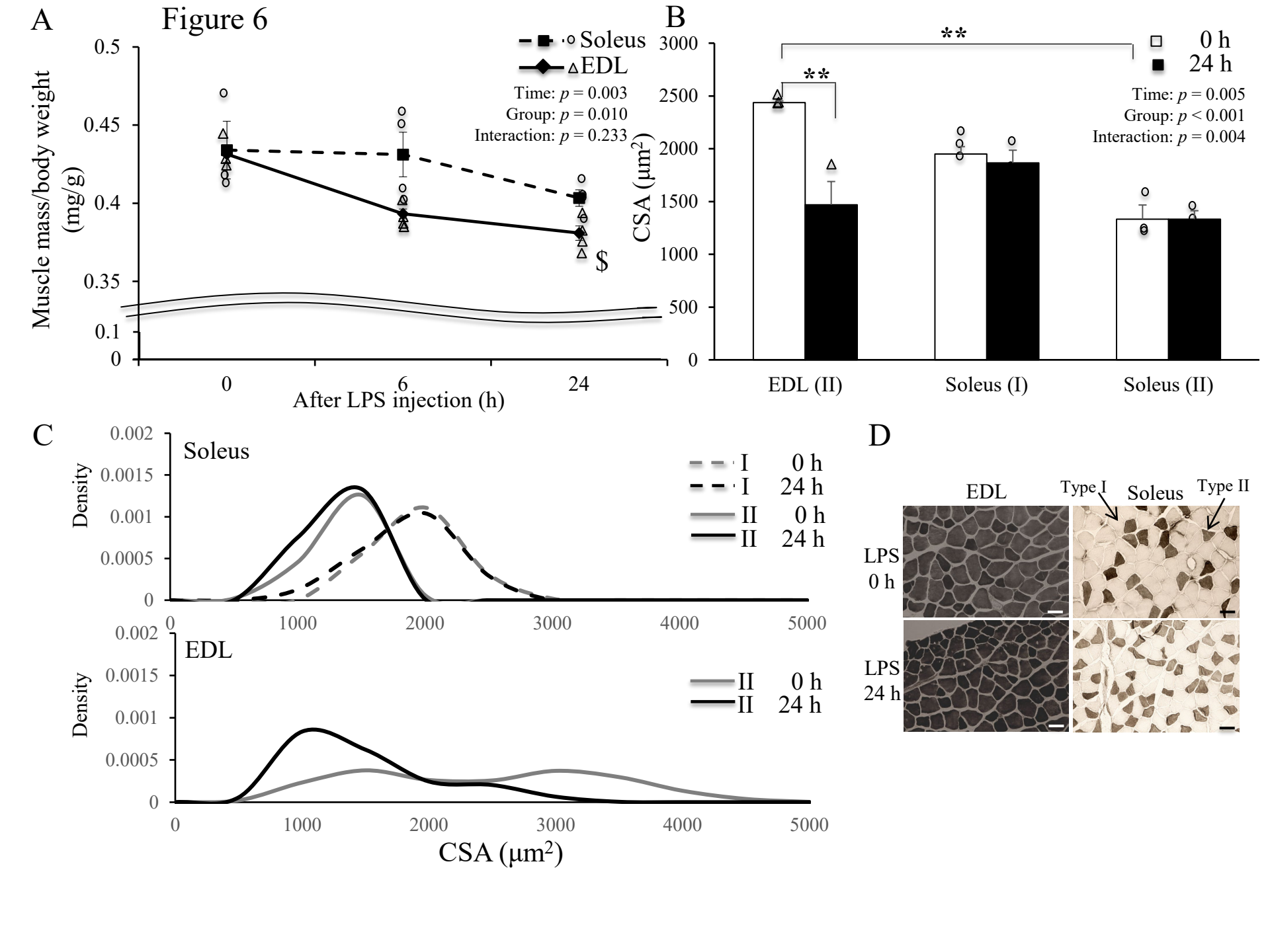
Figure 6
A
Muscle mass/body weight (mg/g)
Soleus
EDL
Time: p = 0.003
Group: p = 0.010
Interaction: p = 0.233
$
After LPS injection (h)
B
CSA (μm2)
0 h
24 h
**
**
Time: p = 0.005
Group: p < 0.001
Interaction: p = 0.004
EDL (II)
Soleus (I)
Soleus (II)
C
Soleus
EDL
Density
I 0 h
I 24 h
II 0 h
II 24 h
CSA (μm2)
D
EDL
Type I
Soleus
Type II
LPS 0 h
LPS 24 h

Figure 7

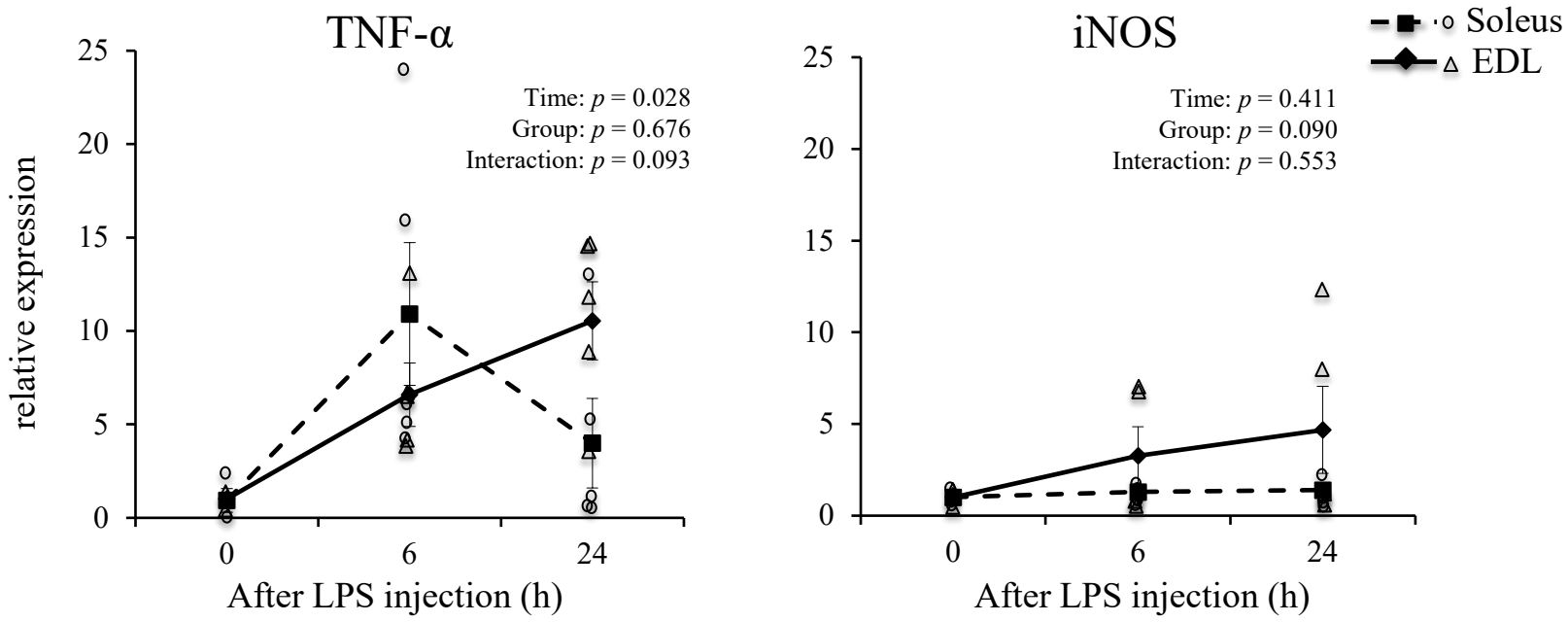
TNF-α
Time: p = 0.028
Group: p = 0.676
Interaction: p = 0.093
relative expression
25
20
15
10
5
0
0
6
24
After LPS injection (h)
iNOS
Time: p = 0.411
Group: p = 0.090
Interaction: p = 0.553
Soleus
EDL
25
20
15
10
5
0
0
6
24
After LPS injection (h)

Figure 8

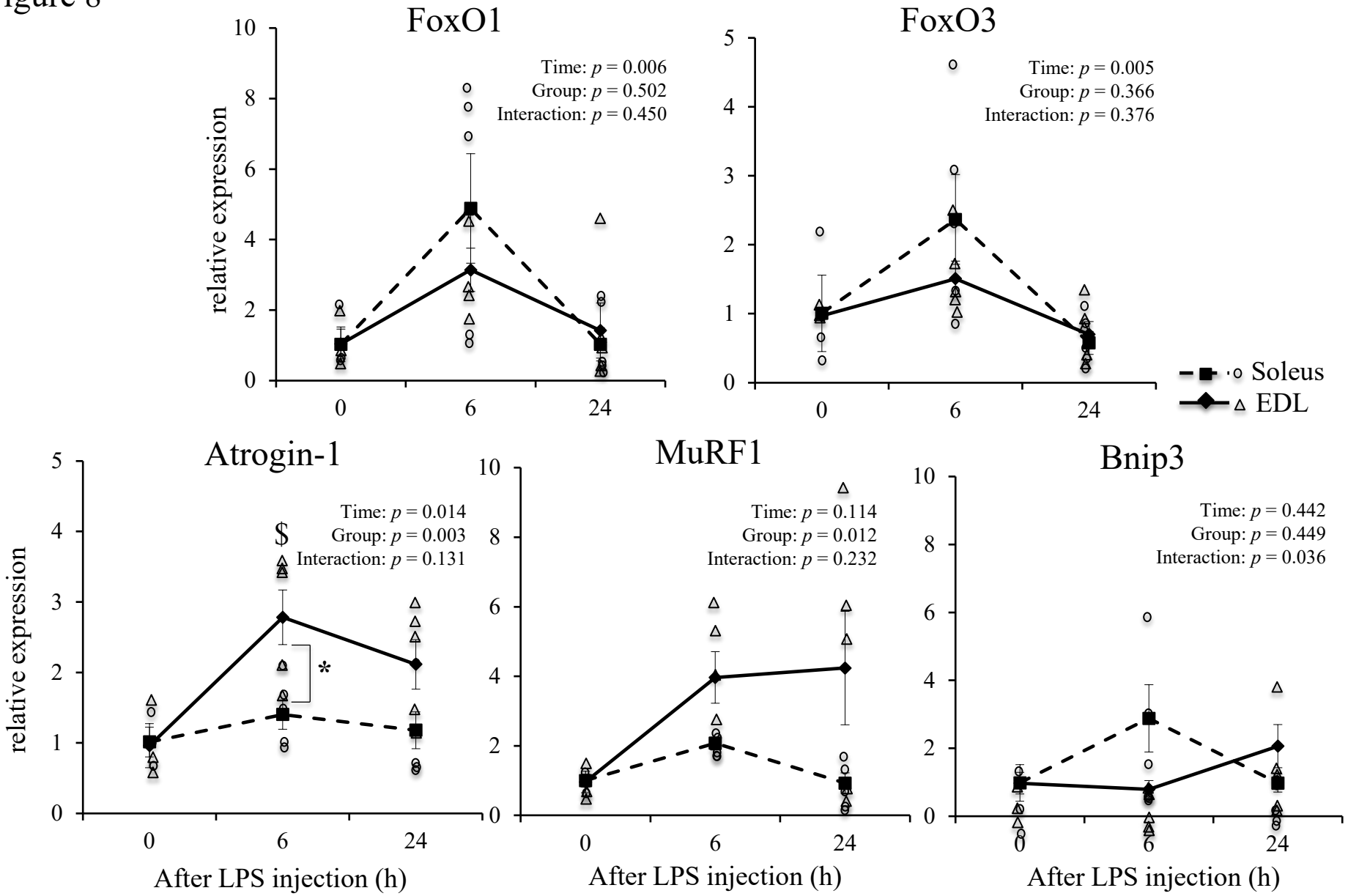
FoxO1
Time: p = 0.006
Group: p = 0.502
Interaction: p = 0.450
relative expression
FoxO3
Time: p = 0.005
Group: p = 0.366
Interaction: p = 0.376
Soleus
EDL
Atrogin-1
Time: p = 0.014
Group: p = 0.003
Interaction: p = 0.131
$
*
MuRF1
Time: p = 0.114
Group: p = 0.012
Interaction: p = 0.232
Bnip3
Time: p = 0.442
Group: p = 0.449
Interaction: p = 0.036
After LPS injection (h)

Table 1. Free fatty acid concentrations (pmol/mg) in soleus and EDL muscles. Data show mean ± SEM ($n = 4$)

	Time after LPS injection								
	0 h		6 h		24 h		*p* value		
	EDL	Soleus	EDL	Soleus	EDL	Soleus	Time	Group	Interaction
Methyl laurate;12:0	3.7 ± 0.8	11.5 ± 8.0	1.0 ± 0.5	1.0 ± 0.4	0.8 ± 0.4	4.5 ± 2.6	0.179	0.227	0.583
Methyl myristate;14:0	8.7 ± 1.7	20.5 ± 4.7	5.3 ± 0.7	11.0 ± 3.1	7. 9 ± 0.5	19.2 ± 4.1	0.103	0.002	0.570
Methyl palmitate;16:0	168.4 ± 20.0	305.6 ± 33.0**	130.7 ± 5.0	197.5 ± 20.2#	191.1 ± 9.8	238.9 ± 22.7	0.011	< 0.001	0.114
Methyl palmitoleate;(Z)16:1n-7	10.2 ± 1.4	34.1 ± 4.7 **	9.6 ± 0.6	27.0 ± 4.8	12.4 ± 1.5	25.6 ± 5.0	0.542	< 0.001	0.350
Methyl stearate;18:0	89.7 ± 11.6	199.5 ± 17.4 **	68.9 ± 4.2	134.6 ± 5.0 **##	122.0 ± 4.2	140.5 ± 13.0 ##	0.004	< 0.001	0.002
Methyl elaidate;(E)18:1n-9	0.6 ± 0.1	1.3 ± 0.8	0.5 ± 0.1	1.4 ± 0.5	0.6 ± 0.1	0.4 ± 0.4	0.443	0.235	0.451
Methyl oleate;(Z)18:1n-9	77.5 ± 8.7	204.1 ± 34.6**	61.9 ± 2.5	125.0 ± 14.6	112.5 ± 10.8	161.0 ± 13.3	0.033	< 0.001	0.095
Methyl linolelaidate;(E)18:2n-6	0.04 ± 0.01	0.31 ± 0.10 **	0.06 ± 0.02	0.25 ± 0.02	0.08 ± 0.00	0.22 ± 0.02	0.827	< 0.001	0.443
Methyl linoleate;(Z)18:2n-6	170.9 ± 35.0	560.2 ± 95.4 **	129.3 ± 16.8	353.9 ± 43.4	258.1 ± 22.1	421.2 ± 41.2	0.067	< 0.001	0.100
Methyl arachisate;20:0	0.7 ± 0.1	1.5 ± 0.2 **	0.5 ± 0.1	0.8 ± 0.0 #	0.6 ± 0.0	1.2 ± 0.2*	0.009	< 0.001	0.275
Methyl ganma-linolenate;(Z)18:3n-6	0.8 ± 0.1	4.3 ± 1.1 **	0.6 ± 0.1	2.3 ± 0.2	0.7 ± 0.1	1.6 ± 0.1	0.025	< 0.001	0.036
Methyl cis-11-icosenoate;(Z)20:1n-9	1.7 ± 0.3	2.4 ± 0.5	1.3 ± 0.1	2.2 ± 0.2	2.9 ± 0.4	3.3 ± 0.2	0.002	0.041	0.701
Methyl linolenate;(Z)18:3n-3	9.9 ± 1.2	32.9 ± 7.8 **	7.3 ± 0.9	22.5 ± 3.7	11.2 ± 1.6	22.3 ± 3.0	0.273	< 0.001	0.329
Methyl cis-11,14-icosadienoate;(Z)20:2n-6	2.9 ± 0.4	6.3 ± 1.0 **	2.6 ± 0.1	4.3 ± 0.4	4.8 ± 0.6	5.4 ± 0.2	0.035	0.001	0.067
Methyl behenate;22:0	0.3 ± 0.0	0.8 ± 0.1 **	0.2 ± 0.0	0.5 ± 0.0 *##	0.2 ± 0.0	0.6 ± 0.1 **	0.001	< 0.001	0.120
Methyl eicosa-8,11,14-trienoate;20:3n-6	3.6 ± 0.9	12.2 ± 1.5 **	3.5 ± 0.5	8.6 ± 0.6 **	6.4 ± 0.2	7.2 ± 0.4 ##	0.108	< 0.001	< 0.001
Methyl erucate;22:1n-9	3.9 ± 1.0	7.7 ± 0.6 **	3.9 ± 0.6	8.3 ± 0.7**	7.3 ± 0.3 $	7.3 ± 0.3	0.075	< 0.001	0.006
Methyl cis-11,14,17-icosatrienoate;(Z)20:3n-3	0.4 ± 0.0	1.3 ± 0.2 **	0.3 ± 0.0	0.5 ± 0.0 ##	0.5 ± 0.0	0.6 ± 0.0 ##	< 0.001	< 0.001	< 0.001

Methyl cis-13,16-docosadienate;(Z)22:2n-6	0.1 ± 0.0	0.4 ± 0.1 **	0.1 ± 0.0	0.2 ± 0.0 ## **	0.3 ± 0.0	0.3 ± 0.0	0.001	0.002	0.006
Methyl lignocerate;24:0	0.3 ± 0.0	1.2 ± 0.1 **	0.3 ± 0.0	0.7 ± 0.1 ## **	0.3 ± 0.0	0.9 ± 0.1 # **	< 0.001	< 0.001	0.011
Methyl cis-7,10,13,16,19-docosapentaenoate;(Z)22:5n-3	152.5 ± 43.3	498.8 ± 57.7 **	127.4 ± 35.4	352.6 ± 20.2 **	253.2 ± 10.4	287.5 ± 6.2 ##	0.073	< 0.001	< 0.001
Saturated fatty acids (SFAs)	271.8 ± 34.0	540.6 ± 54.9 **	206.9 ± 6.0	346.0 ± 27.8 ##	322.9 ± 14.0	405.8 ± 37.3	0.005	< 0.001	0.040
Monounsaturated fatty acids	93.9 ± 11.0	249.7 ± 38.4 **	77.3 ± 2.5	163.9 ± 19.3	135.7 ± 12.5	197.5 ± 17.9	0.054	< 0.001	0.094
Polyunsaturated fatty acids (PUFAs)	413.1 ± 99.4	1476.3 ± 178.1 **	336.6 ± 69.4	977.4 ± 78.3 # **	651.4 ± 36.9	929.2 ± 42.4 ##	0.034	< 0.001	0.003
n-6 Polyunsaturated fatty acids	230.3 ± 50.5	870.3 ± 1113.2 **	188.3 ± 31.6	561.8 ± 54.6 # *	357.8 ± 25.7	578.6 ± 45.3 #	0.041	< 0.001	0.011
n-3 Polyunsaturated fatty acids	182.8 ± 48.9	606.0 ± 69.2 **	148.3 ± 37.9	415.6 ± 26.0 # **	293.6 ± 12.9	350.6 ± 4.2 ##	0.040	< 0.001	0.001
n-6 / n-3 ratio	1.3 ± 0.1	1.4 ± 0.1	1.3 ± 0.1	1.4 ± 0.1	1.2 ± 0.1	1.7 ± 0.1 *	0.485	0.018	0.092
PUFA/SFA ratio	1.5 ± 0.2	2.7 ± 0.2 **	1.6 ± 0.3	2.8 ± 0.2 **	2.0 ± 0.0	2.3 ± 0.1	0.649	< 0.001	0.017
total	778.8 ± 143.0	2266.6 ± 256.3 **	620.8 ± 67.3	1487.3 ± 120.9 # **	1109.9 ± 62.7	1532.5 ± 96.9 #	0.019	< 0.001	0.006

$ $p < 0.05$ versus EDL muscle at 0 h; # $p < 0.05$, ## $p < 0.01$ versus soleus muscle at 0 h; * $p < 0.05$, ** $p < 0.01$ soleus muscle versus EDL muscle, p values indicated the results of two-way ANOVA with time (0, 6, 24 h) and group (soleus versus EDL) as factors.